Role of chemical synapses in coupled neurons with noise

Pablo Balenzuela* and Jordi García-Ojalvo†
Departament de Física i Enginyeria Nuclear, Universitat Politècnica de Catalunya, Colom 11, E-08222 Terrassa, Spain
(Received 22 February 2005; published 1 August 2005)

We examine the behavior in the presence of noise of an array of Morris-Lecar neurons coupled via chemical synapses. Special attention is devoted to comparing this behavior with the better known case of electrical coupling arising via gap junctions. In particular, our numerical simulations show that chemical synapses are more efficient than gap junctions in enhancing coherence at an optimal noise (what is known as array-enhanced coherence resonance): in the case of (nonlinear) chemical coupling, we observe a substantial increase in the stochastic coherence of the system, in comparison with (linear) electrical coupling. We interpret this qualitative difference between both types of coupling as arising from the fact that chemical synapses only act while the presynaptic neuron is spiking, whereas gap junctions connect the voltage of the two neurons at all times. This leads in the electrical coupling case to larger correlations during interspike time intervals, which are detrimental to the array-enhanced coherence effect. Finally, we report on the existence of a system-size coherence resonance in this locally coupled system, exhibited by the average membrane potential of the array.

DOI: 10.1103/PhysRevE.72.021901 PACS number(s): 87.19.La, 87.10+e, 05.40.Ca

I. INTRODUCTION

Neurons are excitable devices that respond in a spiky manner to extrinsic stimuli. These stimuli can be provided by external excitation, by noise, or by neighboring neurons in an extended system [1]. In the absence of deterministic external driving, *isolated* neurons exhibit a spiking behavior purely induced by noise, with the peculiarity that the temporal coherence of the system increases for increasing noise up to a certain noise level, beyond which coherence decreases again. Thus, an optimal amount of noise exists for which coherence is maximal. This phenomenon, which we call *stochastic coherence* (to stress the analogy with the better known stochastic resonance), is known in the literature as coherence resonance or internal stochastic resonance [2,3].

Recent studies have shown that, in extended arrays of neurons, coupling noticeably enhances the stochastic coherence effect [4,5]. This *array-enhanced stochastic coherence* (AESC) has been reported so far, to our knowledge, only in the case of linear (diffusive) electrical coupling, mediated by gap junctions between the neurons [6]. But another very important means of signal transmission between neurons is via chemical synapses, which provide a nonlinear pulsed coupling only when the presynaptic neuron is excited. It is thus of interest to examine the effect of this kind of nonlinear coupling on the stochastic resonance effect described above. Our numerical results, detailed below, show that chemical synapses are more efficient at enhancing coherence than gap junctions. We provide a qualitative explanation for this fact, paying particular attention to the roles of synchronization and of the correlation between neural dynamics in the time lapse between spikes. To that end, we examine the effect of a linear pulsed coupling designed *ad hoc* for this purpose, which exhibits the optimal features of chemical coupling while still acting linearly on the membrane potential during spiking.

II. MODEL DESCRIPTION

A. Neuron model

We consider a one-dimensional array of neurons whose dynamical behavior is described by the Morris-Lecar model [7],

$$\frac{dV_i}{dt} = \frac{1}{C_m}(I_i^{\mathrm{app}} - I_i^{\mathrm{ion}} - I_i^{\mathrm{syn}}) + D_i\xi(t), \tag{1}$$

$$\frac{dW_i}{dt} = \phi\Lambda(V_i)[W_\infty(V_i) - W_i], \tag{2}$$

where $i=1,\ldots,N$ index the neurons, and V_i and W_i represent the membrane potential and the fraction of open potassium channels, respectively. C_m is the membrane capacitance per unit area, I_i^{app} is the external applied current, I_i^{syn} is the synaptic current, and the ionic current is given by

$$I_i^{\mathrm{ion}} = g_{\mathrm{Ca}}M_\infty(V_i)(V_i - V_{Ca}^0) + g_K W_i(V_i - V_K^0) + g_L(V_i - V_L^0), \tag{3}$$

where g_a $(a=Ca,K,L)$ are the conductances and V_a^0 the resting potentials of the calcium, potassium, and leaking channels, respectively. ϕ is the decay rate of W_i, and we define the following functions of the membrane potential:

$$M_\infty(V) = \frac{1}{2}\left[1 + \tanh\left(\frac{V - V_{M1}}{V_{M2}}\right)\right], \tag{4}$$

$$W_\infty(V) = \frac{1}{2}\left[1 + \tanh\left(\frac{V - V_{W1}}{V_{W2}}\right)\right], \tag{5}$$

*Electronic address: pablo.balenzuela@upc.edu; also at Departamento de Física, FCEyN, Universidad de Buenos Aires, Pabellón 1, Ciudad Universitaria (1428), Buenos Aires, Argentina.
†Electronic address: jordi.g.ojalvo@upc.edu

TABLE I. Parameter values of the Morris-Lecar and coupling models used in this work.

Parameter	Morris-Lecar TII
C_m	5 μF/cm^2
g_K	8 μS/cm^2
g_L	2 μS/cm^2
g_{Ca}	4.0 μS/cm^2
V_K	−80 mV
V_L	−60 mV
V_{Ca}	120 mV
V_{M1}	−1.2 mV
V_{M2}	18 mV
V_{W1}	2 mV
V_{W2}	17.4 mV
ϕ	1/15 s^{-1}
Parameter	**Synapses**
α	2.0 ms^{-1} mM^{-1}
β	1.0 ms^{-1}
$T_{\max}$	1.0 mM
g^{syn}	(specified in each case)
τ_{syn}	1.5 ms
E_s	0 mV

$$\Lambda(V) = \cosh\left(\frac{V - V_{W1}}{2V_{W2}}\right), \tag{6}$$

where V_{M1}, V_{M2}, V_{W1}, and V_{W2} are constants to be specified later. The last term in Eq. (1) is a white Gaussian noise term of zero mean and amplitude D_i, uncorrelated between different neurons.

In the absence of noise, an isolated Morris-Lecar neuron shows a bifurcation to a limit cycle for increasing applied current I^{app} [8]. This bifurcation can be a saddle-node (type I) or a subcritical Hopf (type II) bifurcation, depending on the parameters. We chose this last option for the numerical calculations presented in this paper. The specific values of the parameters used are shown in Table I [9]. The equations were integrated using the Heun method [10], which is a second-order Runge-Kutta algorithm for stochastic equations.

B. Coupling scenarios

Most of the studies done so far in the field of stochastic neural dynamics consider linear electrical coupling through gap junctions between adjacent neurons [5,11–15]. But the most common way used by neurons to transmit information is by means of nonlinear pulsed coupling through chemical synapses. In the following paragraphs, we discuss the modeling of the two types of coupling, both of which will be analyzed later.

1. Linear diffusive coupling: Gap junctions

In this kind of coupling, the synaptic current is proportional to the membrane potential difference between a neuron and its neighbors,

$$I_i^{\mathrm{syn}} = \sum_{j \in \mathrm{neigh}(i)} g_{ij}^{\mathrm{syn}}(V_i - V_j), \tag{7}$$

where V_i stands for the membrane potential of neuron i, the sum runs over the neighbors that feed that neuron, and g_{ij}^{syn} is the conductance of the synaptic channel.

2. Nonlinear pulsed coupling: Chemical synapses

In order to take into account the chemical nature of the synapses, we use the model proposed in Ref. [16] to couple the neurons. In this model, the synaptic current through neuron i is given by

$$I_i^{\mathrm{syn}} = \sum_{j \in \mathrm{neigh}(i)} g_i^{\mathrm{syn}} r_j (V_i - E_s), \tag{8}$$

where the sum runs over the neighbors that feed neuron i, g_i^{syn} is the conductance of the synaptic channel, r_j represents the fraction of bound receptors, V_i is the postsynaptic membrane potential, and E_s is a parameter whose value determines the type of synapse (if larger than the rest potential, e.g., E_s=0 mV, the synapse is excitatory; if smaller, e.g., E_s=−80 mV, it is inhibitory).

The fraction of bound receptors, r_j, follows the equation

$$\frac{dr_j}{dt} = \alpha[T]_j(1 - r_j) - \beta r_j, \tag{9}$$

where $[T]_j = T_{\max}\theta(T_0^j + \tau_{\mathrm{syn}} - t)\,\theta(t - T_0^j)$ is the concentration of neurotransmitter released into the synaptic cleft, α and β are rise and decay time constants, respectively, and T_0^j is the time at which the presynaptic neuron j fires, which happens whenever the presynaptic membrane potential exceeds a predetermined threshold value, in our case chosen to be 10 mV. This thresholding mechanism lies at the origin of the nonlinear character of the chemical synaptic coupling, which contrasts with the linear nature of the diffusive electrical coupling of Eq. (7). The time during which the synaptic connection is active is given by τ_{syn}. The values of the coupling parameters that we use [16] are specified in Table I.

III. THE BEHAVIOR OF *N* COUPLED NEURONS: CHEMICAL SYNAPSES VERSUS GAP JUNCTIONS

To obtain a first glimpse of the different effects of chemical and electrical synapses in neural dynamics, we begin by studying the behavior of *two* coupled neurons under the influence of increasing noise intensity D, for the two types of coupling. We fix the external current for the two neurons at I^{app}=46 mA, in such a way that they do not fire in absence of noise. The conductance in the synaptic channels (a measure of the coupling strength) was chosen so that the neurons fire synchronously at least for low noise intensities (g^{syn}=4 nS for chemical synapses and g^{syn}=1 nS for electrical coupling). We use independent realizations of the noise in each neuron but with the same amplitude D.

In the deterministic case (D=0), the system is in a quiescent state. At small but nonzero noise levels, the neurons spike sparsely (albeit synchronously), producing an irregular sequence of well-separated spikes, as can be seen in the top

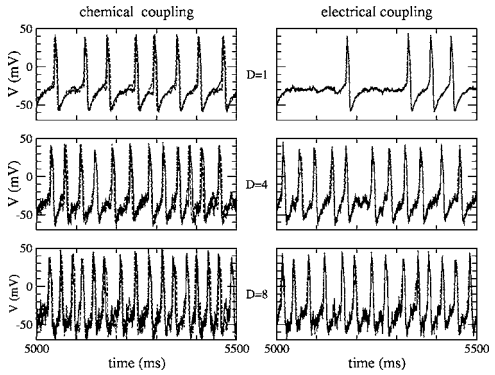

FIG. 1. Membrane potential time traces of two neurons coupled via chemical synapses (left panels) and gap junctions (right panels) for three different noise amplitudes: in the chemical-coupling case $D=0.5$ mV/ms (top), $D=3.5$ mV/ms (middle), and $D=12$ mV/ms (bottom); in the electrical-coupling case $D=1$ mV/ms (top), $D=4$ mV/ms (middle), and $D=12$ mV/ms (bottom). The time series of both neurons are shown as solid and dashed lines (almost indistinguishable in the top right panel). $I^{\mathrm{app}}=46$ mA and $\tau_{\mathrm{syn}}=1.5$ ms in all cases. For chemical coupling, $g^{\mathrm{syn}}=4$ nS (left), whereas for the electrical coupling $g^{\mathrm{syn}}=1$ nS (right).

row of Fig. 1. For an intermediate noise amplitude the spiking rate increases, as does the regularity of the spiking events (middle row in Fig. 1). Finally, for strong noise the spiking of the neurons becomes irregular again (bottom row in Fig. 1). The situation is qualitatively the same for both types of coupling, even though when comparing the most optimal situation in each case, the coherence in the case of chemical coupling is larger than for electrical coupling (as we quantify below). We note that even though the two neurons fire synchronously in both cases, in the chemical-coupling case there exists a slight delay between spikes, and the interspike dynamics are different from each other (cf. the solid and dashed lines in all plots of Fig. 1). In the electrical-coupling case, on the other hand, the time traces are basically identical at all times. This is our first indication that gap junctions are much more efficient than chemical synapses in leading to synchronization.

As usual in neurophysiology, in order to quantify the behavior shown above, we evaluate the time interval between consecutive spikes, T_p, as the main observable in our numerical simulations. In particular, we analyze the first two statistical moments of the distribution of T_p, namely its mean value $\langle T_p \rangle$ and its normalized standard deviation (also known as the coefficient of variation) $R_p=\sigma_p/\langle T_p \rangle$.

Figure 2 plots these two quantities versus noise strength for both chemical and electrical coupling in linear arrays of $N=1$, 2, 10, and 30 neurons, coupled bidirectionally and with periodic boundary conditions. While for both types of coupling the average interspike interval $\langle T_p \rangle$ decays quickly with noise and levels off independently of the system size, the coefficient of variation shows clear differences between chemical and electrical coupling. In the former case, R_p shows a clear trend as N varies, with both its minimum value and the corresponding optimal noise level decreasing steadily (and strongly) with increasing N. For electrical coupling, on the other case, the decrease is less pronounced. For a given system size, the coherence of the chemically coupled array is much better than that of the electrically coupled array.

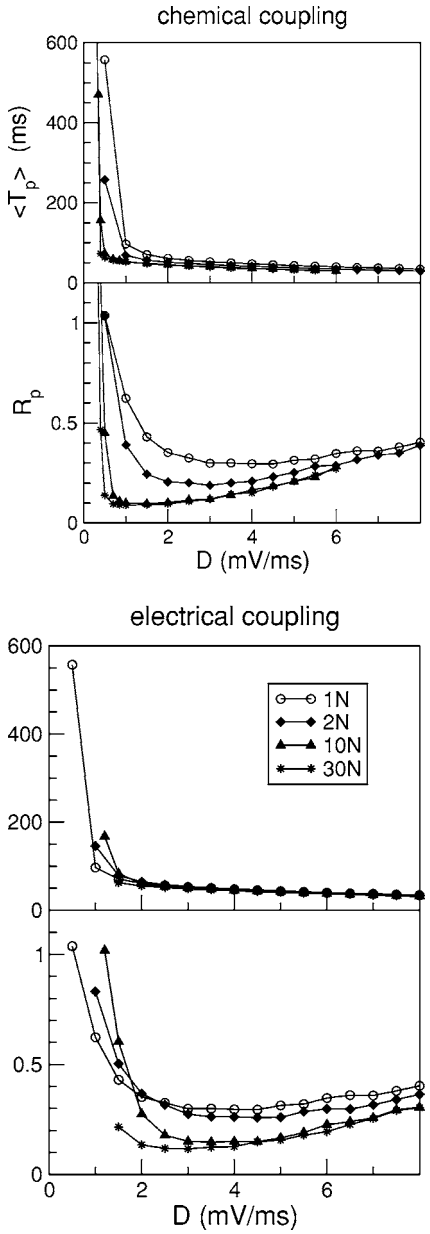

FIG. 2. Mean time interval between spikes $\langle T_p \rangle$ (upper panels) and coefficient of variation $R_p=\sigma_p/\langle T_p \rangle$ (lower panels) for the membrane potential of one neuron coupled via chemical synapses (left panels) and gap junctions (right panels). $I_{\mathrm{app}}=46$ mA and $\tau_{\mathrm{syn}}=1.5$ ms in all cases, whereas $g^{\mathrm{syn}}=4$ nS for the chemical coupling (left) and $g^{\mathrm{syn}}=1$ nS for the electrical coupling (right).

It could be argued that the difference in behavior between the two types of coupling is due to the different coupling coefficients g^{syn} used. But an analysis of the influence of this parameter in each model confirms that chemical coupling is overall more efficient than the electrical one in enhancing coherence. This is evidenced by Fig. 3(a), which plots the minimum coefficient of variation R_p (i.e., its value for optimal noise) versus the coupling coefficient g^{syn} for the two

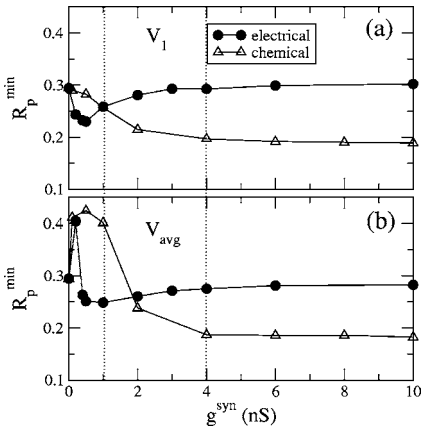

FIG. 3. Minimum coefficient of variation $R_p=\sigma_p/\langle T_p\rangle$ of the local (top) and average (bottom) membrane potential for two coupled neurons vs coupling strength, for both chemical and electrical coupling. $I_{\text{app}}=46$ mA in all cases.

types of coupling in the two-neuron case. It is clear that optimal coherence under electrical coupling is only attainable for a narrow range of coupling strengths. For small and large coupling levels coherence is low, and only for a small intermediate range of coupling strengths is coherence enhanced. On the other hand, for chemical coupling the range of coupling strengths for which coherence is enhanced is much larger, apparently not being bounded from above.

IV. SYNCHRONIZATION AND ARRAY ENHANCEMENT

When choosing the right values of the coupling coefficient that make chemical and electrical coupling comparable, one also needs to take into account the synchronization between the different elements in the array. This can be accomplished via the average membrane potential V_{avg} over all the array. In the case of perfect synchronization, this quantity will exhibit spikes identical to, and simultaneous with, those of the individual neurons. In the case of partial synchronization, spikes in the average potential (defined beyond a given threshold, in our case 10 mV) only occur when a sufficient number of neurons fire within a time window smaller than the spike width. Given these considerations, we determine the interspike interval series of the average potential and compute its statistical properties, namely its mean $\langle T_p\rangle$ and its normalized standard deviation $R_p=\sigma_p/\langle T_p\rangle$.

Figure 3(b) plots the minimum value of R_p (for optimal noise) corresponding to the average potential, for increasing coupling strengths. On the basis of these results, we can establish that the best choices for coupling strengths are $g^{\text{syn}}=1$ nS for electrical coupling and $g^{\text{syn}}\geqslant 4$ nS for chemical. These values are valid not only for two neurons, but for all analyzed system sizes.

We have seen so far that chemical coupling is more effective at enhancing stochastic coherence than electrical coupling. We now discuss the relationship between array-enhanced coherence and synchronization. Array-enhanced coherence is absent for low levels of synchronization, because in that case every neuron behaves as basically uncoupled from all others, so that no constructive effects of coupling (such as array-enhanced coherence) can arise. In the opposite limit, large synchronization levels are not useful in promoting coherence either, since in that case the whole system behaves as a single neuron. However, in the intermediate regime of imperfect synchronization, neighboring neurons can "remind" each other to spike at the right times (i.e., right after the refractory period) for an optimal noise level, so that coherence is globally enhanced. This cannot happen if the neurons are perfectly synchronized.

We now test the efficiency of the two coupling schemes in leading to synchronization. We can already expect, from the functional form of the corresponding coupling term, Eqs. (8) and (9), that chemical synapses will never lead to perfect isochronous synchronization in neuronal arrays. To begin with, the dynamics of the fraction r_j of bound receptors introduces a delay in the interneuronal communication that is absent in the electrical coupling case, Eq. (7). The diffusive form of the latter, furthermore, is compatible with the identical synchronization solution, $V_i(t)=V_j(t)\ \forall i,j$, whereas this is not so for chemical coupling.

To check the previous hypothesis, Fig. 4 compares the mean interspike interval and coefficient of variation of the average potential for the two types of coupling. This figure should be contrasted with the corresponding results for the local membrane potential, Fig. 2. Again, the situation is qualitatively similar in both cases, although there are quantitative differences. The mean time interval between spikes of the average potential increases noticeably for large system sizes (cf. stars in the top row of Fig. 4), but much more for chemical coupling. Also, the coefficient of variation of the interspike interval series becomes more degraded (i.e., the system response is worst at the same system sizes) in the chemical synapse case. These facts indicate that synchronization is worse for chemical than for electrical coupling.

In order to confirm the previous conclusions, we follow how spikes propagate through the array by means of the spike diagram shown in Fig. 5. In this diagram, we plot vertical lines every time that one neuron spikes. In this kind of diagram, synchronized spiking is clearly identified by vertical alignment of the spike markers.

Figure 5 plots the spike diagram for the two types of coupling discussed so far and for $N=2$, 5, 10, and 30 neurons. By comparing the two columns, we can observe that the system with chemical synapses has a charateristic delay time in the propagation of spikes between neurons larger than that corresponding to the electrical coupling. Due to this delay, synchronization is rapidly lost in the case of chemical coupling. For electrical coupling, the spikes also show slight propagation delays, but much smaller than in the chemical case. With the values of coupling constants chosen here, both systems lose synchronicity at similar sizes. If we increased the value of the g^{syn} in the electrical coupling case, the system would remain synchronized for higher system sizes. This would not happen in the chemical case, because there the delay is intrinsic to the synapses and does not depend on the coupling strength. This is a fundamental, qualitative difference between chemical and electrical coupling, which is worth being highlighted.

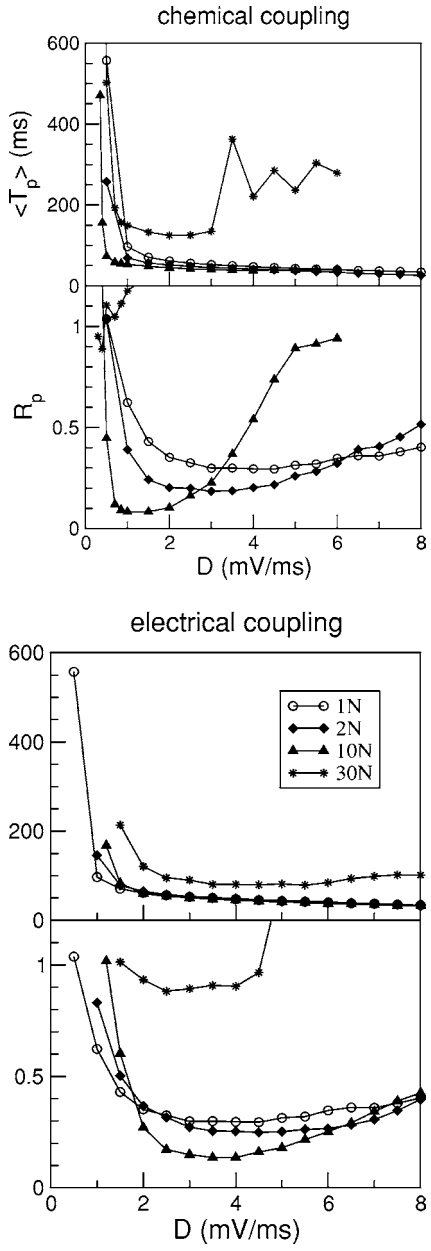

FIG. 4. Mean time between spikes $\langle T_p \rangle$ (upper panels) and coefficient of variation $R_p = \sigma_p / \langle T_p \rangle$ (lower panels) for the average membrane potential and increasing system sizes. Parameters are those of Fig. 2.

V. NONLINEAR VERSUS PULSED COUPLING

There are two main differences between coupling via chemical synapses and gap junctions. First, electrical coupling occurs continuously whereas chemical synapses are only active when the presynaptic neuron spikes. Second, chemical coupling is intrinsically nonlinear, because beyond a certain threshold for the presynaptic neuron, the coupling signal always has the same shape. Which one of these two features leads to enhancement of stochastic coherence reported above for the chemical coupling? We postulate that the relevant feature that makes the chemical synapses more efficient to help neurons to fire is that chemical coupling is

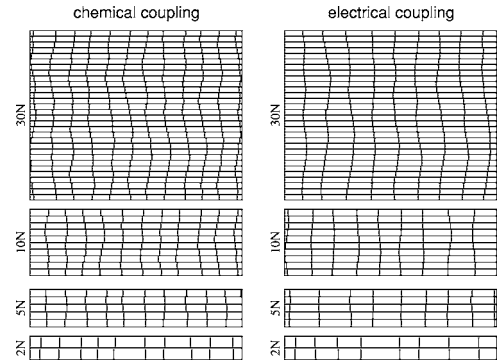

FIG. 5. Spike diagram for N neurons coupled via chemical synapses ($g^{\mathrm{syn}}=4$ nS, left panels) and gap junctions ($g^{\mathrm{syn}}=1$ nS, right panels) for 2, 5, 10, and 30 neurons. $I_{\mathrm{app}}=46$ mA and $D=3$ mV/ms in all cases.

only effective when the presynaptic neuron fires. Otherwise, two neighboring neurons are uncoupled.

To test this hypothesis we couple the neurons with an artificial synaptic current proportional to the difference between the voltages of the coupled membranes (as in the usual linear coupling described in Sec. II B 1), but just during a time τ_{syn} after the presynaptic neuron has fired. This model, which we can call *linear pulsed coupling*, is a hybrid of the two models used above: the coupling is linear with the membrane potential, but the neurons are uncoupled as far as the presynaptic neuron does not fire.

The synaptic current affecting neuron i due to the interaction with its neighbors can be written as

$$I_i^{\mathrm{syn}} = \sum_{j \in \mathrm{neigh}(i)} \theta(T_0^j + \tau_{\mathrm{syn}} - t)\,\theta(t - T_0^j) g_i^{\mathrm{syn}} r_j (V_i - V_j), \tag{10}$$

where $\theta(T_0^j + \tau_{\mathrm{syn}} - t)\,\theta(t - T_0^j)$ is a pulse of width τ_{syn} that turns on when the membrane potential of neuron j is larger that a certain threshold (10 mV in the present case). With this model, a neuron is uncoupled from its neighbors if they are silent, and coupled during a time τ_{syn} after one of them fires.

We also calculate in this case the average time between consecutive spikes, $\langle T_p \rangle$, and its normalized standard deviation $R_p = \sigma_p / \langle T_p \rangle$, both for the spikes produced by the membrane potential of one neuron and for the average membrane potential. The results are plotted in Fig. 6.

Analyzing the results for the local membrane potential (left panel of Fig. 6), we can see that the behavior in this case is similar to (even better than) the case of full chemical coupling: the response of a neuron to a purely noisy excitation is clearly enhanced already when only two neurons are coupled, and rapidly improves with system size, saturating after $N=10$ neurons. Also, the coefficient of variation R_p is as low as for chemical synapses. This happens even though coupling is linear when active.

If we analyze the behavior of the average potential (right panel of Fig. 6), we can see that synchronization holds at even larger system sizes than for the previous natural coupling schemes. In this hybrid model, the $(V_i - V_j)$ term en-

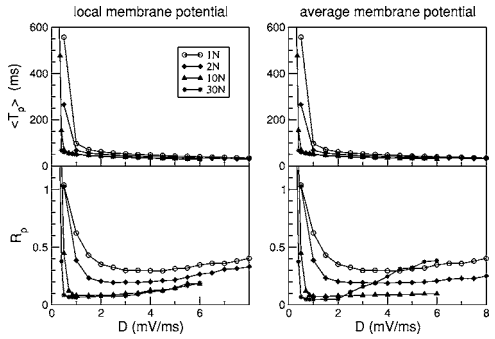

FIG. 6. Mean time between spikes $\langle T_p \rangle$ (upper plot) and coefficient of variation $R_p = \sigma_p / \langle T_p \rangle$ (lower plot) for the membrane potential of one neuron (left panel) and for the average membrane potential (right panel). The neurons are coupled linearly according with expression (10). Parameters are those of Fig. 2 ($g_{\mathrm{syn}}=4$ nS).

hances synchronization for large coupling strengths, but without losing enhancement as in the linear coupling model, due to the inactivation of the coupling in the time elapsed between spikes.

In summary, array-enhanced stochastic coherence is present for linear pulsed coupling. The fact that, in this hybrid type of coupling, this term only turns on when presynaptic neurons fire, supports the hypothesis that the most important feature underneath the efficiency of the coupling is that the neurons remain uncoupled in the absence of firing.

VI. SYSTEM-SIZE COHERENCE RESONANCE

The behavior exhibited in Fig. 4 by the coefficient of variation R_p of the average membrane potential in the chemical-coupling case displays a relevant feature: for small enough noise levels (such as $D=1$ mV/ms), as the system size increases, the regularity of the system increases (i.e., the coefficient of variation decreases), only to degrade again for even larger system sizes. This is a system-size resonance effect. System-size coherence resonance has been recently reported in globally coupled excitable elements [17] and in arrays of neurons interacting via linear diffusive coupling [18]. Here we report it for chemically coupled neurons.

Figure 7 compares the effect of system size on the spike-train coherence for chemically and electrically coupled neurons. Whereas in both cases, the lowest coherence is found for an optimal system size, the effect is more pronounced and occurs at the same system size for the values of g^{syn} chosen.

VII. DISCUSSION

Recent studies have shown that gap junctions are more efficient than chemical synapses in leading to synchronization [19]. The evidence presented in this paper shows that chemical synapses are substantially more efficient than gap junctions in enhancing stochastic coherence in coupled neuron systems. This difference in efficiency stems from the fact that electrical coupling via gap junctions enhances correlations among neurons during interspike time intervals, which prevents neighboring elements to "remind" each other to fire

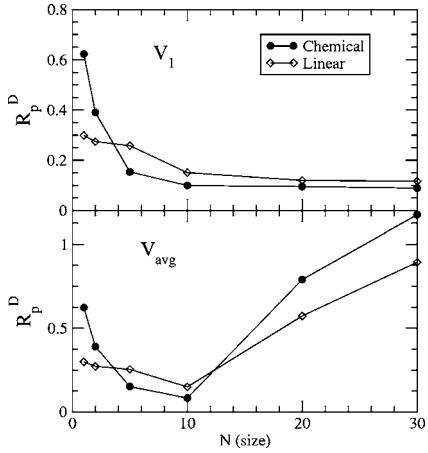

FIG. 7. Coefficient of variation R_p for the membrane potential of one neuron as a function of system size for chemical ($D=1$ mV/ms) and electrical ($D=3$ mV/ms) coupling. $g^{\mathrm{syn}}=4$ nS for chemical coupling and $g^{\mathrm{syn}}=1$ nS for electrical coupling.

at the right time. Chemical coupling, on the other hand, has an intrinsic transmission delay and an intrinsic electrical isolation that degrades this correlation, making that cooperative effect possible. In the simultaneous presence of both types of coupling, we can expect the electrical coupling to prevail, since the neurons will again be coupled at all times.

The different character of both types of coupling is also reflected in the behavior of the neuronal array for increasing coupling strengths (Fig. 3): for electrical coupling, coherence is low only for a narrow window of coupling strengths; for chemical coupling, on the other hand, low coherence arises even if coupling is large. Clearly this difference arises from the fact that for diffusive coupling, large coupling levels lead to high synchronization; for chemical coupling, on the other hand, synchronization does not improve even if coupling strength increases, due to the intrinsic delay.

The present study has only considered excitatory synaptic connections between neurons, because our main interest has been to compare synaptic communication with coupling via gap junctions, which is intrinsically "excitatory." Inhibitory synaptic connections would in principle degrade propagation of the excitations through the neuronal medium. Studies of realistic network architectures combining both excitatory and inhibitory connections are needed, and will be the subject of future work.

Interneuronal communication via chemical synapses is ubiquitous. Its role must therefore be properly assessed when studying stochastic effects in neuronal dynamics. The results presented here show that this type of coupling is in fact beneficial for the coherence of the system.

ACKNOWLEDGMENTS

We acknowledge financial support from MCyT-FEDER (Spain, project BFM2003-07850), and from the Generalitat de Catalunya. P.B. acknowledges financial support from the Fundación Antorchas (Argentina), and from a C-RED grant of the Generalitat de Catalunya.

[1] B. Lindner, J. García-Ojalvo, A. Neiman, and L. Schimansky-Geier, Phys. Rep. **392**, 321 (2004).
[2] A. S. Pikovsky and J. Kurths, Phys. Rev. Lett. **78**, 775 (1997).
[3] B. Lindner and L. Schimansky-Geier, Phys. Rev. E **60**, 7270 (1999).
[4] D. E. Postnov, S. K. Han, T. G. Yim, and O. V. Sosnovtseva, Phys. Rev. E **59**, R3791 (1999).
[5] C. Zhou, J. Kurths, and B. Hu, Phys. Rev. Lett. **87**, 098101 (2001).
[6] J. Keener and J. Snyder, *Mathematical Physiology* (Springer, New York, 1998).
[7] C. Morris and H. Lecar, Biophys. J. **35**, 193 (1981).
[8] M. St-Hilaire and A. Longtin, J. Comput. Neurosci. **16**, 299 (2004).
[9] K. Tsumoto, H. Kitajima, Y. Yoshinaga, K. Aihara, and H. Kawakami, Neurocomputing (to be published).
[10] J. García-Ojalvo and J. M. Sancho, *Noise in Spatially Extended Systems* (Springer, New York, 1999).
[11] S. K. Han, T. G. Yim, D. E. Postnov, and O. V. Sosnovtseva, Phys. Rev. Lett. **83**, 1771 (1999).
[12] A. Neiman, L. Schimansky-Geier, A. Cornell-Bell, and F. Moss, Phys. Rev. Lett. **83**, 4896 (1999).
[13] O. Kwon and H.-T. Moon, Phys. Lett. A **298**, 319 (2002).
[14] C. Zhou, J. Kurths, and B. Hu, Phys. Rev. E **67**, 030101(R) (2003).
[15] E. Ullner, A. Zaikin, J. García-Ojalvo, R. Báscones, and J. Kurths, Phys. Lett. A **312**, 348 (2003).
[16] A. Destexhe, Z. F. Mainen, and T. J. Sejnowski, Neural Comput. **6**, 14 (1994).
[17] R. Toral, C. R. Mirasso, and J. D. Gunton, Europhys. Lett. **61**, 162 (2003).
[18] M. Wang, Z. Hou, and H. Xin, ChemPhysChem **5**, 1602 (2004).
[19] N. Kopell and B. Ermentrout, Proc. Natl. Acad. Sci. U.S.A. **101**, 15482 (2004).